First Principles Investigation of Mineral Component of Bone: CO_3 Substitutions in Hydroxyapatite

R. Astala* and M. J. Stott

Department of Physics, Queen's University, Kingston, Ontario K7L 3N6, Canada

Received March 8, 2005. Revised Manuscript Received May 6, 2005

First principles calculations are used to investigate carbonated hydroxyapatite, a naturally occurring mineral and also the inorganic component of animal bone. Two types of carbonate substitution are studied: A-type in which the carbonate ion substitutes for an OH and B-type where the substitution is for a phosphate. Both types have unbalanced charges and various forms of charge compensation are treated. The methods, which are based on density functional theory and first principles pseudopotentials, yield equilibrium atomic arrangements, changes in lattice parameters, and total energies for different types of substitution. When calculated energies of selected stable compounds are used, the formation energies of different carbonate substitutions with accompanying charge compensation defects can be compared. The results indicate that compact complexes are energetically favored, and a B-type material with charge compensation by a calcium vacancy together with a hydrogen atom which bonds to a neighboring phosphate is the most stable of all those considered.

I. Introduction

Hydroxyapatite (HA), $Ca_5(PO_4)_3OH$, is a naturally occurring rare mineral,[1] but its most common occurrence is as the main inorganic constituent of natural bone. In addition, with silicon doping it is the basis of bioactive ceramics which show promise as bone repair materials. HA has a hexagonal structure with space group $P6_3/m$ and lattice parameters $a = b = 9.4225$ Å and $c = 6.8850$ Å.[2] There are two formula units per unit cell and the arrangement is typical of the calcium apatites and can be viewed as consisting of unconnected, robust PO_4^{3-} tetrahedra with Ca^{2+} in the space between and a chain of OH^- ions along the *c*-axis to balance the charge (Figure 1). Monoclinic structures with four formula units per unit cell have also been reported,[1,3−6] where the monoclinic unit cell is obtained from the hexagonal one by doubling the *b* lattice parameter and by having different arrangements of the anion chains. Difficulties in obtaining the stoichiometric compound, particularly with regard to the OH content, may influence the structure. The structure of the hexagonal phase of HA presents a problem. Following failed attempts to fit X-ray diffraction data using the space group $P6_3$, the structure was found with space group $P6_3/m$ through the addition of two mirror planes perpendicular to the [001] and passing through $z = 1/4$ and $z = 3/4$. However, this structure has four possible sites for the two OH groups per unit cell, a difficulty which was resolved by assuming 0.5 occupancy per site resulting from disorder in every anion column or disorder from column to column.[7] The atomic arrangement and the electronic structure of HA along with other apatites has recently been studied using total energy first principles methods,[8] and the purpose of this paper is to report results of a similar study of the form of HA found in natural bone.

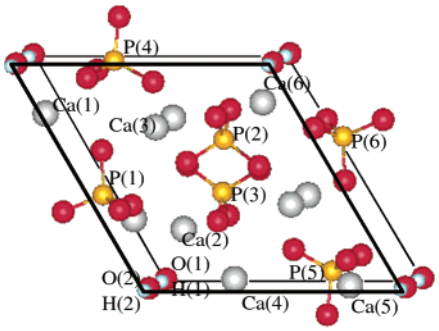

Figure 1. Hydroxyapatite structure viewed along the *c* axis. The numbers indicate the defect sites, as listed in Table 1. Note that the numbers are arbitrary labels that do not correspond to the crystallographic notation. The colors are as follows: oxygen (red), phosphorus (yellow), calcium (gray), and hydrogen (light blue).

Animal bone divides broadly into two components, the fibrous organic collagen matrix into which the inorganic crystalline component forms. The latter is a nonstoichiometric hydroxyapatite containing impurities, which are believed to be important for biological functions.[9] Principal among these is 4−7 wt % carbonate.[10,11] This mineral component has a hexagonal crystal structure and is in the form of platelets with average length and widths of 500 × 250 Å with the *c*-axis lying in the plane of the plate, and between 15 and 40 Å thick.[12] Little is firmly established about the atomic arrangements in natural bone because of the small size of

* To whom correspondence should be addressed. E-mail: astala@physics.queensu.ca.

(1) Elliott, J. C. *Structure and Chemistry of the Apatites and Other Calcium Orthophosphates*; Elsevier: Amsterdam, 1994.
(2) *Standard Reference Materials Program (https://srmors.nist.gov)*; National Institute of Standards and Technology: Gaithersburg, MD, 2003.
(3) Morgan, H.; Wilson, R. M.; Elliott, J. C.; Dowker, S. E. P.; Anderson, P. *Biomaterials* **2000**, *21*, 617.
(4) Ikoma, T.; Yamazaki, A.; Nakamura, S.; Akao, M. *J. Solid State Chem.* **1999**, *144*, 272.
(5) Elliott, J. C.; Mackie, P. E.; Young, R. A. *Science* **1973**, *180*, 1055.
(6) Haverty, D.; Tofail, S. A. M.; Stanton, K. T.; McMonagle, J. B. *Phys. Rev. B* **2005**, *71*, 094103.
(7) Kay, M. I.; Young, R. A. *Nature* **1964**, *204*, 1050.
(8) Calderín, L.; Stott, M. J.; Rubio, A. *Phys. Rev. B* **2003**, *67*, 134106.
(9) Posner, A. S. *Physiol. Rev.* **1969**, *49*, 760.
(10) Weiner, S.; Traub, W. *FASEB J.* **1992**, *6*, 879.
(11) Dorozhkin, S. V.; Epple, M. *Angew. Chem., Int. Ed.* **2002**, *41*, 3131.

10.1021/cm050523b CCC: $30.25
Published on Web 07/02/2005

the crystals, but synthetic carbonated apatites and the related minerals dahllite and francolite are well-studied. The carbonate ions are held to occupy two types of sites depending on the manufacture. In most high-temperature apatites the CO_3^{2-} resides at an OH^- ion site termed an A-type substitution, whereas in the low-temperature materials the CO_3^{2-} replaces a PO_4^{3-} ion, the so-called B-type substitution. Although much experimental work has been reported using X-ray and neutron diffraction, infrared and electron spin resonance spectroscopies, thermal decomposition, and nuclear magnetic resonance studies, uncertainties remain in the details of the chemical composition, location, and orientation of the CO_3^{2-} ions and the nature of any associated defects providing charge compensation.[1,9,13−19]

A CO_3^{2-} ion substituting for either an OH^- ion in the A-type material or a PO_4^{3-} ion in B-type constitutes a charged defect, and it is expected that there will be considerable lowering of the energy and much increased stability if an additional charged defect is associated with the CO_3^{2-} to provide local charge compensation. For A-type, the charge compensation can take place by OH vacancies. For B-type material, combinations of OH and Ca vacancies as compensating defects have been proposed, and self-compensation by having both A- and B-site carbonate substitutions is possible.[1,13] For the AB-carbonate apatite, a combination of two V_{Ca} and one V_{OH} per three B-site CO_3 ions was observed,[13] where V_{Ca} denotes a Ca vacancy and likewise for the hydroxide vacancy. Furthermore, there is experimental evidence of HPO_4^{2-} groups in carbonate HA, which can act as compensating species.[15,20] Simulations are performed to investigate a number of possible charge compensation mechanisms and the energetically favorable ones are identified. Changes in lattice parameters as a function of carbonate concentration have been reported for synthetic material prepared in different ways and the results of the simulations casts light on these effects.

In a single-crystal X-ray diffraction study of A-type material, a configuration in which the CO_3 apical direction is parallel to the *c*-axis, leading to space group $P\bar{6}$ was reported.[21] However, in more recent Fourier transform infrared spectroscopy (FTIR) and single-crystal X-ray diffraction study, a configuration where the CO_3 apical direction is close to perpendicular to the *c*-axis and the ion plane is canted by about 12° was found.[19,22] At the B-site, different structural models have been investigated, including configurations in which the C impurity is at different locations relative to the PO_4 tetrahedron it is replacing. Such configurations include the sloping face of the PO_4 tetrahedron, the plane parallel to the (001) plane near the center of the tetrahedron, or the side of the tetrahedron that is parallel to the *c* axis.[23] In the case of Na_{Ca} substituted carbonate apatite, and in the case of francolite—fluoride containing carbonate apatite— the CO_3 plane forms an angle of about 30° to the *c*-axis.[23] In FTIR and single-crystal X-ray diffraction studies similar observations were made for AB-type carbonate apatite; also, a third configuration for A-site CO_3 was found in a high-pressure-synthesized material.[19,24] In a neutron powder diffraction study a substitution on the mirror plane of the PO_4 tetrahedron was proposed.[25] However, in an X-ray powder diffraction study of calcium-deficient carbonate HA it was reported that the C ion occupies the side of the tetrahedron parallel to the *c* axis.[26]

First principles methods are able to provide some information on local atomic arrangements but we are aware of only a few such studies. One is a study of A-type carbonated apatite using a cluster consisting of a six Ca and six PO_4 fragment of HA.[27] The electronic ground state was treated at the Hartree−Fock level and only the structure of the CO_3^{2-} was relaxed. This pioneering work found the plane of the CO_3^{2-} ion oriented at an angle of 7° to the crystallographic *c*-axis when the absence of the other OH^- in the cluster provides charge compensation. The results support A-site configuration where the CO_3 apical direction is close to perpendicular to the *c* axis, but the lack of any account of electron correlation and the rigidity of the atomic environment in these calculations require attention. A comparison of electron nuclear double-resonance results and DFT-based cluster calculations within the local spin density approximation for CO_2 and CO_3 A-site substituted HA was performed in ref 28. These calculations provided information about the chemical environment of the defect. However, to study the energetics, atomic geometries, and volume changes for different defects, periodic supercell calculations with relaxed geometries are required.

We have investigated different possible arrangements of the CO_3^{2-} ion in both A- and B-type carbonated HA. These calculations are based on density functional theory for treating the effects of electron−electron interactions, and use first principles pseudopotentials for the electron−ion interactions. The atoms of interest occupy one or more HA units cells and the structure is repeated to form a superlattice. The electronic structure and the positions of all atoms and the cell parameters are relaxed so that the electron ground state is obtained for the equilibrium arrangement of the atoms. Similar calculations were performed earlier for stoichiometric HA,[8] giving good agreement with experiment.

(12) Weiner, S.; Wagner, H. D. *Annu. Rev. Mater. Sci*. **1998**, *58*, 271.
(13) Driessens, F. C. M.; Verbeeck, R. M. H.; Kiekens, P. Z. *Anorg. Allg. Chem.* **1983**, *504*, 195.
(14) Taylor, M. G.; Parker, S. F.; Simkiss, K.; Mitchell, P. C. H. *Phys. Chem. Chem. Phys.* **2001**, *3*, 1514.
(15) Mkukuma, L. D.; Skakle, J. M. S.; Gibson, I. R.; Imrie, C. T.; Aspden, R. M.; Hukins, D. W. L. *Calcif. Tissue Int.* **2004**, *75*, 321.
(16) Loong, C.-K.; Rey, C.; Kuhn, L. T.; Combes, C.; Wu, Y.; Chen, S.-H.; Glimcher, M. J. *Bone* **2000**, *26*, 599.
(17) Cho, G.; Wu, Y.; Ackerman, J. L. *Science* **2003**, *300*, 1123.
(18) Driessens, F. C. M. *Z. Naturforsch., C: J. Biosci.* **1980**, *35*, 357.
(19) Fleet, M. E.; Liu, X.; King, P. L. *Am. Miner.* **2004**, *89*, 1422.
(20) Wu, Y.; Glimcher, M. J.; Rey, C.; Ackerman, J. L. *J. Mol. Biol.* **1994**, *244*, 423.
(21) Suetsugu, Y.; Takahashi, Y.; Okamura, F. P.; Tanaka, J. *J. Solid State Chem.* **2000**, *155*, 292.
(22) Fleet, M. E.; Liu, X. *J. Solid State Chem.* **2003**, *174*, 412.
(23) Wilson, R. M.; Elliott, J. C.; Dowker, S. E. P.; Smith, R. I. *Biomaterials* **2004**, *25*, 2205.
(24) Fleet, M. E.; Liu, X. *J. Solid State Chem.* **2004**, *177*, 3174.
(25) Leventouri, T.; Chakoumakos, B. C.; Papanearchou, N.; Perdikatsis, V. *J. Mater. Res.* **2001**, *16*, 2600.
(26) Ivanova, T. I.; Frank-Kamenetskaya, O. V.; Kol'tsov, A. B.; Ugolkov, V. L. *J. Solid State Chem.* **2001**, *160*, 340.
(27) Peeters, A.; Maeyer, E. A. P. D.; Alsenoy, C. V.; Verbeeck, R. M. H. *J. Phys. Chem. B* **1997**, *101*, 3995.
(28) Schramm, D. U.; Terra, J.; Rossi, A. M.; Ellis, D. E. *Phys. Rev. B* **2000**, *63*, 024107.

The paper is structured as follows. A description of the method appears next. This includes a summary of the computational techniques and parameters used and describes the structures used for modeling carbonate substitution. These are followed by the results in the third section, where we present data concerning the energetics and geometries of different defects. Finally, in the fourth and fifth sections, we give discussion and conclusions.

II. Methods

The structures were modeled using electron structure density functional theory[29,30] with SIESTA software.[31] The GGA-PBE approximation for exchange-correlation energy was employed,[32] and the valence orbitals were represented using a localized basis set. Troullier-Martins norm conserving pseudopotentials[33] were used to describe the electron−ion interactions. The valence orbital basis set was as follows. For Ca ions, semicore 3s, and valence 4s and 3p orbitals were included. The 3s and 3p were treated with single ζ (SZ) orbitals, while double ζ with a polarization orbital (DZP) was used for the 4s. For O ions, double ζ (DZ) 2s and triple ζ with polarization orbitals (TZP) 2p were used. For P, DZ 3s and DZP 3p orbitals were used, and for H DZP 1s orbitals were used.

A large basis set was required for C to obtain reasonably well converged results. A TZP was used for 2s and a triple ζ with two polarization orbitals for 2p. As a technical aside, the valence wave functions for the C pseudo atom have a long tail so that a large cutoff radius (6 Bohrs) for the first ζ orbitals was required. Also, the addition of a 2s polarization orbital lowered the total energy by adding more variational freedom to the basis set in the tail region. The exigencies for triple ζ orbitals for C have been reported earlier for amorphous carbon systems.[34]

The Ca, P, O, and H pseudopotentials and the Ca, P, and H basis functions were tested and used in earlier studies of hydroxyapatite[8] and tricalcium phosphates.[35] The C pseudopotential was tested by comparing atomic excitation energies to all-electron results, and together with C and O orbitals, by calculating formation energies of diamond, O_2, CO, and CO_2 systems. Also, an isolated CO_3^{2-} ion, both in spin unpolarized and in the spin-1 state, was relaxed using a large supercell and neutralizing background charge. The results changed little when the supercell size was increased, indicating that the interaction of the ion with its images was not significant and that the simulation was a good representation of the ion in vacuo. For carbonated apatites, superlattice geometries were used, in which the atomic substitutions of interest were made in one or multiple HA unit cells. The Brillouin zone was sampled using Monkhorst-Pack grids so that the *k*-point density was at least 0.08 $Å^{-1}$.[36] Equilibrium structures were obtained by relaxing all atom coordinates and the lattice parameters.

A. A-Site Substitution. Different substitution mechanisms were examined. In the A-site substitution CO_3^{2-} occupies an OH^--site in the channel. A natural way for compensating the excess charge is to introduce an OH^- vacancy on the neighboring OH site in the channel. This case was treated in the cluster calculation in ref 27 where the plane of the CO_3^{2-} ion after relaxation was found parallel to the *c* axis or almost so. In the hexagonal host crystal this allows for 12 configurations: either one or the other OH ion is substituted, and at each OH site there are three possible CO_3 orientations differing by 120° rotations around the *c* axis. Finally, the presence of two mirror planes doubles the number of possible configurations. But, there may be disordered arrangements of the CO_3^{2-} ions in which the orientation varies from one unit cell to its neighbor.[1] We have considered two possibilities. First, an ordered CO_3^{2-} arrangement, with one CO_3^{2-} impurity in a single HA unit cell; this breaks the 3-fold symmetry of HA. Second, a spiral arrangement was treated, in which a stack of three HA unit cells in the *c* direction was used as a host crystal, and three CO_3^{2-} ions were placed on every other OH-site so that their orientation progressed by 120° from one cell to the next up the stack. The latter model was used as an attempt to estimate the effect of disorder on the total energy.

Table 1. Impurity and Vacancy Sites in Different Configurations, Using the Labeling Convention of Atoms for Pristine HA Shown in Figure 1[a]

	C site	V_O site	V_H site	
site A ordered	O(1),H(1)	O(2)	H(2)	
site A spiral	O(1),H(1)	O(2)	H(2)	
	C site	V_O site	V_H site	V_{Ca} site
site B1(a)	P(1)	O(2)	H(2)	Ca(1)
site B1(b)	P(1)	O(1)	H(1)	Ca(2)
site B1(c)	P(2)	O(2)	H(2)	Ca(2)
site B1(d)	**P(2)**	**O(2)**	**H(2)**	**Ca(3)**
		C site	C site	V_{Ca} site
site B2(a)		P(3)	P(4)	Ca(3)
site B2(b)		P(3)	P(5)	Ca(4)
site B2(c)		P(3)	P(5)	Ca(5)
site B2(d)		P(3)	P(6)	Ca(5)
clustered B2(c)		P(3)	P(5)	Ca(5)
site B2(c), first CO_3 separated		P(3 4+*c*)	P(5)	Ca(5)
site B2(c), second CO_3 separated		P(3 4)	P(5+*c*)	Ca(5)
site B2(c), V_{Ca} separated		P(3)	P(5)	Ca(6+*c*)
isolated C impurity		P(3)		
isolated Ca vacancy				Ca(6)
		C site		H_{Ca} site
site B3(a)		P(3)		Ca(6)
site B3(b)		P(3)		Ca(6)
site B3(c)		P(3)		Ca(3)
site B2(d)		P(3)		Ca(2)
isolated H_{Ca}				Ca(6)

[a] The "+*c*" denotes that the defect occupies an equivalent site in a neighboring unit cell in the *c* direction. The most stable structure in each category has been underlined.

B. B-Site Substitution. In the B-site substitution the CO_3^{2-} occupies a PO_4^{3-} site. Three charge compensation mechanisms were considered. First, compensation of a single CO_3^{2-} can be achieved by removing an OH^- and a Ca^{2+} (denoted a B1-complex). Second a complex of two CO_3^{2-} impurities can be compensated by a single Ca^{2+} vacancy (denoted a B2-complex). Third, compensation of a single CO_3^{2-} can be achieved by a H atom placed at a Ca vacancy (denoted B3-complex). With each of these types of B-site substitution, there are a number of symmetry inequivalent ways to arrange the impurities and vacancies. Furthermore, at a given site, the CO_3^{2-} ion has orientational degrees of freedom, especially whether its plane is parallel or perpendicular to the *c* axis.[23] Instead of treating all possible configurations, we discerned trends in the defect formation energies from a small subset of configurations. The impurity and vacancy sites for the different A- and B-complexes that have been treated are listed in Table 1. The sites are labeled according to atom positions in pure HA which are identified in

(29) Hohenberg, P.; Kohn, W. *Phys. Rev.* **1964**, *136*, B864.
(30) Kohn, W.; Sham, L. *Phys. Rev.* **1965**, *140*, A1133.
(31) Ordejón, P.; Artacho, E.; Soler, J. *Phys. Rev. B.* **1996**, *53*, R10441.
(32) Perdew, J. P.; Burke, K.; Ernzerhof, M. *Phys. Rev. Lett.* **1996**, *77*, 3865.
(33) Troullier, N.; Martins, J. L. *Phys. Rev. B* **1991**, *43*, 1993.
(34) Nelson, J. S.; Stechel, E. B.; Wright, A. F.; Plimpton, S. J.; Schultz, P. A.; Sears, M. P. *Phys. Rev. B* **1995**, *52*, 9354.
(35) Yin, X.; Stott, M. J.; Rubio, A. *Phys. Rev. B* **2003**, *68*, 205205.
(36) Monkhorst, H. J.; Pack, J. D. *Phys. Rev. B* **1974**, *13*, 5188.

Table 2. Defect Energies per CO_3^{2-} at Different Sites, Relative to the Most Stable Structure Overall, B2(c), and in Parentheses, to the Most Stable Configuration with Same Charge Compensation Mechanism[a]

	ΔE (eV)
site A ordered	+2.36 (0)
site A spiral	+2.42 (+0.06)
site B1(a)	+2.10 (+0.00)
site B1(b)	+2.21 (+0.11)
site B1(c)	+2.10 (0)
site B1(d)	**+2.10 (+0.00)**
site B2(a)	+0.73 (+0.43)
site B2(b)	+0.41 (+0.11)
site B2(c)	+0.30 (0)
site B2(d)	+0.99 (+0.69)
site B2(c), clustered double cell	+0.77 (+0.47)
site B2(c), first CO_3 separated	+0.70 (+0.40)
site B2(c), second CO_3 separated	+0.82 (+0.52)
site B2(c), V_{Ca} separated	+1.38 (+1.08)
isolated CO_3 parallel to *c* and V_{Ca}[b]	**+6.07 (+5.77)**
isolated CO_3 in 32° to *c* and V_{Ca}[b]	**+5.65 (+5.35)**
site B3(a)	+1.32
site B3(b)	+0.59
site B3(c)	+0.57
site B3(d)	0
isolated CO_3 and H_{Ca}	+5.82

[a] The most stable structure in each category has been underlined. [b] Ca vacancy at column site.

Figure 1. For the B1-complex four different configurations, B1(a), B1(b), B1(c), and B1(d), for B2-complex, four configurations, B2(a), B2(b), B2(c), and B2(d), and for B3-complex, four configurations, B3(a), B3(b), B3(c), and B3(d), were relaxed. The initial orientations of the CO_3^{2-} ions, that is, the orientations prior to relaxation, are given below. In all the B1- and B2-complexes, the CO_3^{2-} ion planes were initially set parallel to the *c* axis, with the exception of B2(d), where they were inclined. In the B3(a) the C O_3^{2-} ion plane was set close to parallel to *c*. The B3(b) configuration was similar but with the CO_3^{2-} ion plane set perpendicular to *c*. Also, in all the other B3-complexes, the CO_3^{2-} ion plane was set close to perpendicular to *c*.

In hydroxyapatite, the Ca ions occupy either columns aligned in the *c*-direction (Ca_1 site) or triangles surrounding the OH channel (Ca_2 site). To investigate the difference between Ca vacancies on these two possible sites, the Ca was removed from the column site (Ca(3) in Figure 1) in the B1(d), B2(a), and B3(c) complexes, while in the other complexes the Ca was removed from the triangle site. Table 4 lists the initial distances between the impurities and their compensating defects. The coordinates of Ca vacancies and H_{Ca} impurities were taken to be those of the missing Ca ions in pristine HA; in the case of V_{OH}, the position of the O atom was used.

Electrostatic energy considerations alone would suggest that the substituting CO_3^{2-} ion and the associated charge compensating defects should be in close proximity. However, other considerations which might compete are lattice strain and opportunities for bonding. The effects of the degree of clumping together of the CO_3^{2-} and the associated defects were investigated by considering three cases involving the B2(c)-complex. In these either one of the CO_3^{2-} ions or the V_{Ca} was moved far away from the rest of the B2(c)-complex. This was done using a stack of two HA unit cells in the *c*-direction, and by moving the defect to the neighboring cell.

C. Isolated Defects. The limiting case of defects being far removed from one another was investigated using double cells of HA. In electron- and hole-compensated systems such as are expected for these isolated charged defects, weakly localized states can form at the defect. To correctly treat such states and to reduce the spurious interactions between neighboring defects brought on by the enforced superlattice periodicity, large supercells are required. It was for this reason that cells doubled in the *c*-direction were used for the isolated defects. One case had a single CO_3^{2-} ion in a double cell, a second case had a V_{Ca} in a double cell, and a third treated a H_{Ca} defect similarly. With V_{Ca}, both column site and triangle site vacancies were investigated, and with H_{Ca}, the calcium was removed from the triangle site. For the isolated CO_3^{2-} ion, the two configurations were used, in which the CO_3^{2-} plane was either close to perpendicular or parallel to *c*. These systems were relaxed and the energies per double cell were used in the following combinations to estimate the total energy of the dispersed components of the different complexes in an HA lattice

$$2 \times (CO_3^{2-} - HA) + (V_{Ca} - HA) - 5 \times HA$$

and

$$(CO_3^{2-} - HA) + (H_{Ca} - HA) - 3 \times HA$$

These energies were then used with the total energy for the complexes in HA to obtain the binding energies of the various complexes. For V_{Ca}, the column site vacancy supercell energy was used as it was found to be slightly lower than the energy of the triangle site vacancy. It should be noted that in all the other calculations the lattice parameters as well as all atom coordinates were relaxed, but for the isolated defects they were fixed at the calculated values for pure HA to simulate better the dilute conditions.

D. Formation Energy. Of special interest are the relative energies of different defect complexes. However, the total energies of the structures having different substitution mechanisms cannot be compared directly because of differences in stoichiometry. A rigorous comparison of the defect formation energies would require knowledge of chemical potentials μ of individual atoms so that the reference energy can be decomposed as

$$n(\mathrm{Ca})\mu(\mathrm{Ca}) + n(\mathrm{P})\mu(\mathrm{P}) + n(\mathrm{O})\mu(\mathrm{O}) + n(\mathrm{H})\mu(\mathrm{H}) + n(\mathrm{C})\mu(\mathrm{C}) \quad (1)$$

where $n(X)$ denotes the number of atoms of species X.[37] Unfortunately, these chemical potentials are difficult to obtain. Instead, stable intermediate compounds can be used to balance the stoichiometry. These include dicalcium phosphate hydrate (brushite, $CaHPO_4 \cdot 2H_2O$), hydrated lime [$Ca(OH)_2$], and H_2O molecules in a vacuum. The use of intermediate compounds to compare energies amounts to an approximation of the chemical potentials. The total energies per formula unit for the different intermediate systems used here were calculated using the same ingredients and methods employed in the carbonated HA systems. As a starting point for the optimization of brushite, a structure reported in ref 38 was used.

The A-site substitution and the B1-complex are linked by a reaction involving brushite and water

$$CO_3{-}HA(\text{A-site}) \rightleftarrows CO_3{-}HA(\text{B1-site}) + CaHPO_4 \cdot 2H_2O - 3H_2O \quad (2)$$

whereas the B1- and B2-complexes are linked by a reaction involving $Ca(OH)_2$ and pristine hydroxyapatite

$$2CO_3{-}HA(\text{B1-site}) \rightleftarrows CO_3{-}HA(\text{B2-site}) + Ca_{10}(PO_4)_6(OH)_2 - Ca(OH)_2 \quad (3)$$

The B1- and B3-complex are linked by a simple reaction involving

(37) Laks, D. B.; de Walle, C. G. V.; Neumark, G. F.; Pandelites, S. T. *Phys. Rev. Lett.* **1991**, *66*, 648.
(38) Sainz-Díaz, C. I.; Villacama, A.; Otálora, F. *Am. Miner.* **2004**, *89*, 307.

Table 3. Lattice Parameters of Different Structures[a]

	CO_3 wt %	*a* (Å)	*b* (Å)	*c* (Å)	α (deg)	*β*(deg)	*γ* (deg)
pristine hydroxyapatite	0	9.72	9.72	7.15	90.0	90.0	120.0
hydroxyapatite, experiments		9.4176		6.8814			120
A, ordered	5.8	+0.16	−0.03	−0.01	+0.9	−0.4	−1.3
A, spiral	5.8	+0.12	+0.13	+0.01	−0.0	−0.0	+0.1
A, experiments		+0.139	*b*∼2*a*	−0.009			+0.36
B1(a)	6.3	−0.20	−0.03	+0.04	−0.3	−0.0	−0.8
B1(b)	6.3	−0.20	−0.01	+0.08	+2.1	−1.7	+0.7
B1(c)	6.3	+0.03	−0.20	+0.03	+0.3	+0.0	−0.3
B1(d)	**6.3**	**−0.09**	**−0.10**	**−0.03**	**−2.3**	**+2.7**	**−1.0**
B2(a)	14.7	−0.08	−0.10	−0.13	−0.3	−0.0	−0.1
B2(b)	14.7	−0.12	−0.26	+0.10	−1.2	+0.7	+0.6
B2(c)	14.7	−0.05	−0.31	−0.02	+1.0	+0.3	−0.7
B2(d)	14.7	−0.16	−0.19	+0.02	−1.6	+0.7	+0.5
clustered site B2(c)	6.6	−0.06	−0.16	+0.05	+0.3	+0.4	−0.3
B2(c), first CO_3 separated	6.6	−0.06	+0.15	+0.02	−0.2	+0.3	−0.4
B2(c), second CO_3 separated	6.6	−0.07	+0.10	+0.02	+0.1	−0.1	+0.0
B2(c), V_{Ca} separated	6.6	−0.07	−0.17	+0.14	+0.4	+0.5	−0.1
B3(a)	6.2	−0.23	−0.15	+0.06	+0.1	−0.1	−1.4
B3(b)	6.2	−0.22	−0.18	+0.09	+1.4	−2.4	−1.5
B3(c)	6.2	−0.03	−0.07	−0.02	+0.5	−1.1	−0.2
B3(d)	6.2	−0.21	+0.03	−0.02	+0.3	+0.1	−1.1
B, experiments[b]	6.2, 6.3, 6.6	−0.03−0.00		0.01−0.02			
B, experiments[c]	14.7	−0.05		0.02			

[a] For pristine HA, absolute values, and for the substituted structures, changes (in Å) are given. The experimental data for A-site carbonate is for a pseudohexagonal structure with doubled *a* parameter.[1] The most stable structure in each category has been underlined. [b] Experimental data for 6.2, 6.3, and 6.6 wt % is interpolated from Table 4.6 in ref 1. The changes for these three concentrations are the same within the accuracy used here. [c] This entry is extrapolated from entry 1 in Table 4.6 in ref 1.

Table 4. Initial Distances between Defect and Compensating Sites; Calculated for Corresponding Sites in Pristine HA Structure[a]

	C−V_O (Å)	C−V_{Ca} (Å)	V_O−V_{Ca} (Å)
site B1(a)	3.73	3.57	2.46
site B1(b)	4.99	3.16	4.12
site B1(c)	3.73	3.57	2.46
site B1(d)	3.73	3.33	5.98

	C−C (Å)	C−V_{Ca} (Å)	C−V_{Ca} (Å)
site B2(a)	5.16	3.71	3.33
site B2(b)	4.86	3.16	3.58
site B2(c)	4.86	7.01	3.79
site B2(d)	5.64	7.01	6.39
clustered site B2(c)	4.86	7.01	3.79
site B2(c), first CO_3 separated	8.65	7.02	3.79
site B2(c), second CO_3 separated	8.65	7.01	3.81
site B2(c), V_{Ca} separated	4.86	7.99	7.91

	C−H_{Ca} (Å)
site B3(a)	3.57
site B3(b)	3.57
site B3(c)	3.71
site B3(d)	3.79

[a] The most stable structure in each category has been underlined.

just H_2O

$$CO_3{-}HA(B1\text{-site}) + H_2O \rightleftarrows CO_3{-}HA(B3\text{-site}) \quad (4)$$

Defects that have the same compensation mechanism but different concentrations can be compared using a reaction

$$CO_3{-}HA(\text{dilute}) \rightleftarrows CO_3{-}HA(\text{concentrated}) + n\text{HA} \quad (5)$$

where the number of HA unit cells (*n*) is chosen to balance the composition on the two sides.

III. Results

The results of the calculations for the isolated carbonate ion are presented first. Then, the results concerning the energetics of the different substitution types and the various modes of charge compensation are given. This allows the systems to be ranked according to their formation energies and the most stable configurations can be established. The comparison is done using the reaction equations (2), (3), (4), and (5) presented in the previous section. After the most stable configuration is identified, attention turns to the results concerning the defect clustering for this system, calculated using double unit cells or uncompensated defects. Finally, the detailed atomic geometries and lattice parameter changes for different structures are presented, with a focus on the most stable complexes.

The isolated CO_3^{2-} ion prefers the spin unpolarized state by 3.9 eV, compared with the spin-1 state. The ion in the spin unpolarized configuration is planar, with C−O bond lengths of 1.33 Å and O−C−O angles of 120°. The ion is larger than the OH^- but smaller than PO_4^{3-}; in pristine hydroxyapatite the calculated P−O distance is about 1.6 Å and the O−H distance 0.98 Å.

A. Energetics. The defect energies are presented in Table 2. The ordered single-cell substitution of A-site CO_3^{2-} impurities was found to be more stable by 0.06 eV than the spiraling arrangement. However, the energy difference is small and may not be significant, but it does indicate that the interactions between the CO_3^{2-} impurities in neighboring cells are weak. It is noteworthy that the lattice parameters for the spiraling arrangement deviate less from those of bulk hydroxyapatite than those for the single-cell substitution, and the hexagonal unit cell shape is nearly preserved.

For the B1-complex, the (c) configuration was found to be the most stable, but the (a) configuration had almost the same energy. In the (a) configuration, the OH^- and Ca^{2+} vacancies are tightly clustered compared with the (b) and (c) configurations. Also, the lattice parameters are closest to the pure HA values.

In the case of the B2-systems, the (c)-type configuration was found to be the most stable. In this arrangement, one of the CO_3^{2-} ions is rather distant from the Ca vacancy, while the other one is close. To test the possibility that moving the second CO_3^{2-} further away from the Ca vacancy might lower the energy, the configuration (d) was investigated. However, this led to an increase in the total energy. For the B3-complex, the (d)-type configuration, in which the CO_3^{2-} and the H_{Ca} are in different Ca−P layers, is the most favorable.

The reaction energies between A- and B1-substitutions, and between B1- and B2-substitutions, were calculated using reaction equations (2) and (3), respectively. The results show that, for the most stable configurations, the A- and B1-type substitutions are close together in energy, with the reaction energy favoring the B1-type by 0.32 eV. The B2-substitution is clearly preferred over B1, with a reaction energy of 1.80 eV. The B3-substitution is even more favored over B1, with a reaction energy of 2.10 eV. Thus, it follows that the B3-substitution is the most energetically favored of these four substitutions and charge compensation arrangements.

The B-type carbonate HA systems discussed so far have been rather concentrated with a complex in every HA cell. More dilute B2(c) systems were investigated by taking one complex with the defects clustered together in one-half of a double HA cell and the other half undoped. The energy of the B2(c)-complex was found to increase significantly in the double cell. The energies of the different complexes also changed when the defects comprising the complex were dispersed. The energy either increased or decreased slightly depending on which CO_3^{2-} ion was displaced when the distance between the impurities increased. Moving the V_{Ca} away from the CO_3^{2-} to the neighboring unit cell led to an increase in the total energy of the system by 1.1 eV. At the limit of very large separation simulated using two supercells with uncompensated defects, the defect formation energy increased substantially, by 4.9 eV relative to the complex in the double cell. Similarly, for the B3-substitution, separating the CO_3^{2-} and H_{Ca} into isolated cells increased the energy by 5.8 eV. The accuracy of these numbers is somewhat suspect because of the possibility of spurious interactions between periodic images. However, it is unlikely that any such errors would change the qualitative result that there is a large energy penalty for separating CO_3^{2-} from the compensating V_{Ca} or H_{Ca}.

B. Atomic Geometries and Lattice Parameters. The internal coordinates of the CO_3^{2-} ions relax slightly on both OH^- and PO_4^{3-} sites. Typically the ion retains a planar geometry with about 120° O−C−O angles and the C−O bond lengths of about 1.3 Å (Table 5). The CO_3^{2-} ion in HA as for the gas phase ion is significantly smaller than the PO_4^{3-} group and larger than the OH^- ion. As we shall see, this has consequences on the lattice parameters. On the A-site, the orientation of the normal to the CO_3^{2-} plane is roughly perpendicular to the *c* axis, making an angle of about 80° for the single-cell substitution. The relaxed structure is shown in Figure 2. For the triple-cell spiraling configuration, the angles are about 85−86°, in reasonable agreement with the orientation found in earlier H−F cluster calculations.[27] The CO_3^{2-} is oriented so that one CO_3^{2-} apical direction is close to perpendicular to the *c* axis, in agreement with the theoretical prediction in ref 27, as well as with experimental data in refs 22 and 19, but differing from experimental results in ref 21, where the apical direction was parallel to *c*. Note that the parallel configuration was close to metastable and careful relaxations were required to obtain the minimum energy configuration.

On B-sites, the orientation changed greatly as the atomic positions and lattice parameters are allowed to relax. The final geometries for the most stable structures for each kind of substitution mechanism are shown in Figures 3, 4, 5, and 6. In the B2(c)-configuration, the CO_3^{2-} ion planes are closer

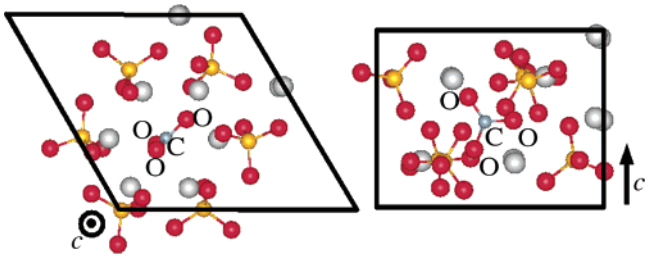

Figure 2. The single-cell A-site substitution with CO_3^{2-} located in the *c*-aligned channel. On the left the top view and on the right the side view with CO_3^{2-} between the PO_4^{3-} layers are shown. The small gray sphere denotes the carbon atom.

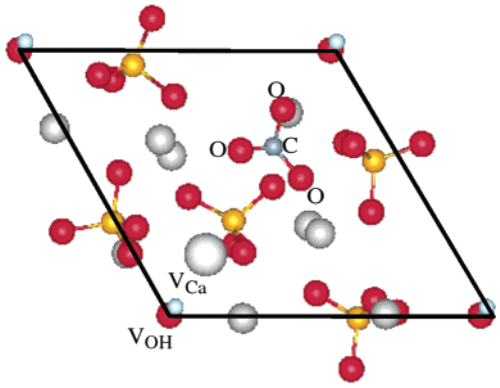

Figure 3. The B1(c)-complex. The large gray sphere shows the location of the vacant Ca site.

Table 5. Geometries of Low Energy Configurations and Multiple Unit Cell Systems of Impurities[a]

	d(C−O) (Å)	∠O−C−O (deg)
site A ordered	1.28−1.31	116.0−123.7
site A spiral	1.28−1.31	117.6−124.2
site B1(c)	1.27−1.34	116.8−121.6
site B2(c)	1.28−1.33	117.0−121.9
clustered site B2(c)	1.30−1.32	118.4−121.3
site B2(c), first CO_3 separated	1.30−1.31	119.1−120.7
site B2(c), second CO_3 separated	1.30−1.31	118.5−120.9
site B2(c), V_{Ca} separated	1.29−1.32	117.9−121.9
site B2(d)	1.29−1.32	118.4−121.5
uncompensated, CO_3 parallel to *c*	1.30−1.32	118.8−120.2
uncompensated, CO_3 at 32° to *c*	1.30−1.32	119.3−120.6

[a] The C−O distances and O−C−O angles are tabulated.

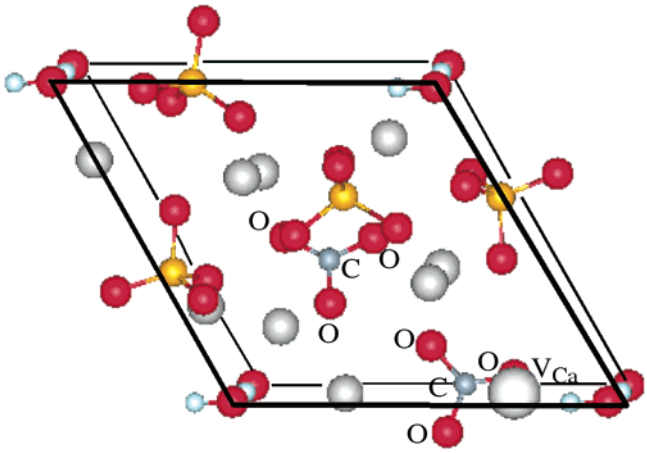

Figure 4. The B2(c)-complex. The large gray sphere shows the location of the vacant Ca site.

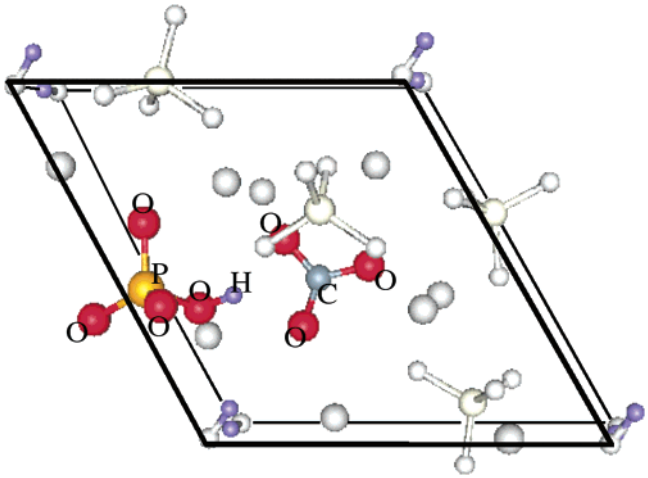

Figure 5. The B3(d)-complex. The HPO_4^{2-} and CO_3^{2-} groups are highlighted.

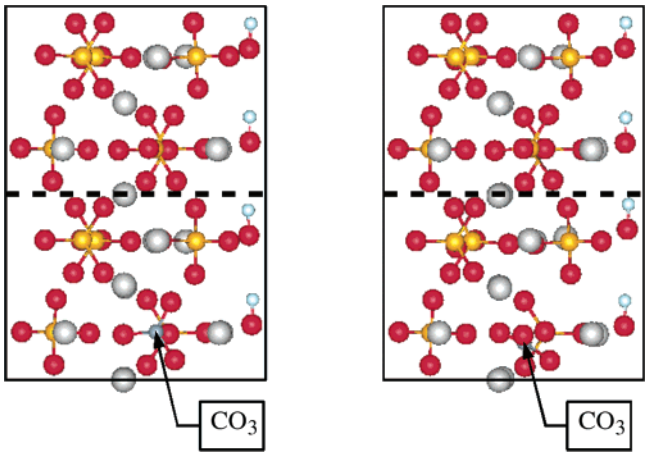

Figure 6. The uncompensated carbonate HA double-cell structures, viewed down the [110] axis. On the left, the CO_3^{2-} ion plane is parallel to the *c* axis, while on the right it is inclined.

to parallel to *c*. The angles are about 36° for the P(4) site substitution and 6° for the P(10) site. The former is in agreement with the conclusions drawn from polarized IR measurements on single crystals of francolite.[1] Similar agreement was found for the isolated uncompensated CO_3^{2-} in a double cell, where the angle is about 32°. For the B3(d)-configuration, the plane of the CO_3^{2-} ion is close to parallel to the (001) crystal plane, making an angle of about 4° with it. In our calculations, the configurations in which the CO_3^{2-} plane is close to perpendicular or inclined to *c* tend to have lower energy than the configurations where it is parallel. This is clearly seen by comparing the energies of parallel and perpendicular configurations of uncompensated CO_3^{2-} in a double cell, and also the B3(a) and B3(b) configurations where the main difference is the CO_3^{2-} orientation. It was also found that, in most of the cases where the CO_3^{2-} plane was initially set parallel to *c*, with exception of one of the carbonates in the B2(a) configuration and the B3(a) configuration, the ion tended to relax toward inclined or perpendicular configurations. These results support the conclusions of refs 1, 19, 23, and 24 for francolite, and Na_{Ca} and AB-substituted carbonate apatite, where the C was found to occupy sloping faces of PO_4 tetrahedra it was replacing.

Another prominent feature of the atomic relaxations in the B2(c)-configuration is the relaxation of the OH group that is nearest to the calcium vacancy. Instead of pointing in the *c* direction as in pure HA, the OH intermolecular axis points almost in the *a* direction, so that the H is closer to the vacancy. Such a relaxation can be understood to stem from electrostatic interactions, with the positive end of the OH dipole approaching the negative V_{Ca}. Similar behavior is observed when more dilute double unit cell substitutions are investigated. This effect was also detected in the B3(d) configuration. The results show that the OH ion has substantial rotational freedom in the channel.

The behavior of lattice parameters for relaxed structures is presented in Table 3. The comparison of experimental and calculated results shows a systematic overestimation in the calculated values which is typical when GGA exchange correlation functionals are used and may reflect the sensitivity of the values to the choice of basis set, but the changes in lattice parameters from the HA values are expected to be reliable. With the A-site substitution, the *a* and *b* lattice parameters were found to increase. The observed hexagonal symmetry is best preserved in the spiraling A-site substitution. For this system the *a* lattice parameter was found to expand by 1.2% and the *b* by 1.3%; the *c* parameter changed very little, increasing by only 0.1%. This agrees well with the experimental result which shows an increase of 1.4% in *a* and a 0.1% decrease in *c*. It should be noted that the A-site doping level in the experimental sample was typically about 0.9−0.95% CO_3^{2-} per HA unit cell, slightly less that the maximum of one.[1]

In contrast, for B1-, B2-, and B3-site substitutions the *a* and *b* lattice parameters were found to decrease, on average by 1−2%, for the most stable structures. The lattice parameters approach pure HA values for double unit cells that have the lower defect concentration. In most cases the *c* parameter changed only slightly. The experimental data for B-site substituted material shows a small decrease in *a* and an increase in *c*, so that while the calculations predict the correct trend they overestimate the lattice contraction. Unfortunately, because the exact ratio of OH and Ca vacancies in the experimental samples is not known, a comparison with our calculated data is somewhat unreliable. For the most stable structures, the unit cell volumes increased by 2.6% for both the ordered and spiral A-site complex and

decreased by 1.1% for the B1- and B3-complexes and by 3.3% for the B2-complex. This difference between B2 versus B1 and B3 stems from the higher CO_3 concentration for B2-complex; the volume decrease for the B2-complex is reduced to 1.5% in the doubled unit cell in which the concentration is halved.

In the most stable B-site substitutions, the triangle Ca site for the V_{Ca} was energetically preferred over the column site, though in the case of B1-site substitutions the energy difference was negligible. In the isolated V_{Ca}, the column site vacancy has slightly lower (0.11 eV) energy.

The calculations showed the B3(d)-complex to be the most energetically favorable. The relaxed complex is shown in Figure 5. In this system the H atom preferred to bond with an O in a nearby PO_4 group, forming a HPO_4 ion. This bonding will have contributed to the large binding energy for the system. The O−H distance was 1.02 Å, which is slightly longer than the O−H distance of 0.98 Å for the channel OH groups in undoped HA. Also, the P−(OH) bond length at 1.68 Å was longer then the P−O distance of about 1.6 Å in pure HA, indicating that the protonation weakened the P−O bond. The geometry of the HPO_4 group differs from those we found for the relaxed brushite structure. The bond lengths in brushite were slightly different with shorter P−(OH) distances of 1.66 Å and longer O−H distances of 1.03 Å. More prominently, the distortion indices that measure the deviation of the six O−P−O angles (θ_i) from the ideal tetrahedron value [$\theta_0 = \cos^{-1}(-1/3)$] showed noticeable differences. The distortion index can be defined either as root-mean-square difference

$$D_{\mathrm{RMS}} = \sqrt{\frac{1}{6}\sum_{i=1}^{6}(\theta_i - \theta_0)^2} \tag{6}$$

or as an absolute value difference

$$D_{\mathrm{ABS}} = \frac{1}{6}\sum_{i=1}^{6}|\theta_i - \theta_0| \tag{7}$$

In both cases the HPO_4 in the B4(d) complex was more distorted, having values of $D_{\mathrm{RMS}} = 4.06$ and $D_{\mathrm{ABS}} = 3.52$, while for brushite HPO_4 groups the respective values were $D_{\mathrm{RMS}} = 3.72$ and $D_{\mathrm{ABS}} = 3.31$.

IV. Discussion

The large cost in energy of about 6 eV to separate completely the CO_3^{2-} from its charge compensating defects for the B-type substitution suggests strongly that for small carbonate doping there will be local charge neutrality with the carbonate and the compensating defects forming a rather compact complex; this is expected for a large band-gap material (calculated Kohn−Sham eigenvalue gap over 5 eV)[8] for which electron or hole charge compensation is likely to be energetically unfavorable. However, in natural bone and the synthetic materials for which experimental data is available the concentrations of carbonate are such that there is on average one or more carbonate per two HA cells, and there will always be charged defects rather close to any carbonate. The comparison of total energies for the most stable structures for the different types of compensation mechanisms implies that the B3-complex where the CO_3^{2-} is compensated by H_{Ca} is energetically favored over the others that have been considered. The B2-complex, where two CO_3^{2-} ions are compensated by V_{Ca}, is also fairly stable, being only 0.3 eV higher in energy. But the carbonate concentration when the whole complex is in a single HA unit cells is double that for the B3-complex, and if the complex is placed in a double HA cell so that the concentration is the same as for the B3-complex, the energy increases by a further 0.4−0.5 eV and the B2-complex becomes less of a contender.

The high energy cost of A-site substitution is surprising since this material is commonly synthesized. Setting aside uncertainties in the comparisons of energies for different stoichiometries and in the individual total energies themselves, it is possible that A-site substitution is kinetically favored, with the complex formation occurring by simple diffusion along the *c*-aligned channel. Furthermore, OH vacancies could be plentiful, in readiness for the A-type substitution, if the processing is at high temperature in low humidity. In contrast, the B-site substitutions we have considered involve phosphate and calcium vacancies and the formation of the complex may be slower. The behavior of CO_3^{2-} is close to that of a rigid ion so that the O−C−O bond angles stay close to 120°, while the bond lengths relax somewhat. The CO_3^{2-} is smaller than the PO_4^{3-} and consequently it can change its orientation when occupying such a site. On the A-site, the configuration of the carbonate ion is such that the CO_3^{2-} plane is close to parallel to the *c*-axis and an apical direction is perpendicular to *c*. On the B-site, the carbonate prefers configurations where the CO_3^{2-} plane is perpendicular or inclined to the *c*-axis.

The trends in the lattice parameters can be largely accounted for by ion size arguments. The CO_3^{2-} is larger than the OH^- ion but smaller than PO_4^{3-}, and so an increase in lattice parameters over the pure HA values is expected for A-site substitution and a decrease for B-type material. The volumes of both A-type systems were found to increase by about 2.6%, and for the most stable B-type systems there was a contraction of 1−2% for the cases where there was on average one carbonate per HA cell. However, the volume change depended on the compactness of the complex and decreased in magnitude when the B2 complex was dispersed. Also, there was a decrease in contraction when the V_{Ca} was separated slightly from the rest of the B2-complex. The substitutions were often accompanied by substantial distortions of the hexagonal HA unit cell. This is due to the small size of the systems that have been considered, mainly one HA cell, and at most three cells together, with the ordered superlattice geometry. These restrictions preclude a proper treatment of impurity disorder that would tend to preserve the hexagonal structure. The distortion is less pronounced when the defects are diluted by doubling the unit cell, and also in the case of the spiraling A-site substitution where the effect of disorder has been simulated to some extent. The spiraling arrangement leaves the unit cell shape very close to hexagonal. The expansion of the *a* lattice parameter for this arrangement is in excellent agreement with experimental results. Furthermore, the close agreement between the total

energies of the ordered single cell and the spiraling A-site substitution suggests that the neighboring CO_3^{2-} ions do not interact strongly. In the case of B-site substitutions the *a* and *b* lattice parameters typically decrease more than seen in the experiments. However, a comparison is not straightforward because it is not known what charge compensation mechanisms took place in the experimental samples.

In the case of the B3-complex, the most energetically favored, for which hydrogen plus a calcium vacancy provide charge compensation, the H ion being much smaller than the Ca ion is able to relax away from its initial position at the Ca site and bond with nearby O atoms. Consequently, this defect can be considered either as a H_{Ca} impurity or as a complex formed by V_{Ca} and interstitial H. The H ion is likely to be mobile, making its experimental detection difficult. However, HPO_4 groups in bone mineral have been experimentally detected;[20] these groups are different from the HPO_4 groups in brushite, which is in agreement with our results regarding the HPO_4 distortion indices. The energy preference for H_{Ca} charge compensation may result from two factors: first, no completely vacant lattice sites are present, and second, the formation of a PO_4-H bond lowers the energy.

The total energy results for the double unit cell arrangements of B2-configurations indicate that reducing the impurity concentration is energetically unfavorable. With CO_3^{2-} ions occupying B-sites, the *a* and *b* lattice parameters tend to contract which may lead to lattice parameter mismatch with surrounding pure hydroxyapatite. In dilute carbonate material the lattice would be strained due to this mismatch between the doped and undoped regions of the crystal, leading to a higher defect formation energy. This may be the case in the configuration where the $2\ CO_3^{2-} + V_{Ca}^{2-}$-complex is clustered in one-half of the double cell while the other half is pure HA. The CO_3^{2-} ions do not have a strong tendency to cluster as separating one of them from the rest of the complex does not lead to much of an energy change and the calculations suggest that the energy could actually decrease. However, there is an energy penalty for separating the V_{Ca} from the rest of the complex.

The calculations reported here are for extended systems and in addition to the periodicity imposed on the system, making it difficult at present to model disordered systems, there is no free surface. While this may not be a serious limitation in the modeling of synthetic carbonated HA, the modeling of natural bone may be another matter. Bone HA is in the form of crystalline platelets extended along the *c*-axis direction, which lies in the plane of the plate, and with the *b*-axis perpendicular to the plate. But the plates are a mere 15−40 Å thick so that any carbonate dopants with their associated charge-compensating defects are within 10 Å or so of a (010) surface which must influence the energetics of the different charge compensation mechanisms and which locations for complexes are favored. The presence at the surface of the crystallite of body fluid rather than vacuum is a further complicating factor. For example, if a B3 complex is near the interface of bone and body fluids, the H may diffuse to the interface, leading to a charged surface or, across the interface protonating a species in the fluid or catalyzing reactions.[9] Furthermore, because B1- and B3-complex are related by a simple hydration reaction, it is possible that the B1-complexes are more likely to be found at low H_2O partial pressure. First principles methods are sufficiently well-developed for simulations of atomic behavior at these interfaces to be attempted.

The calculations give the total energy for an atomic arrangement and the forces on the atoms. The atom positions are then relaxed until static equilibrium is attained. The nuclei are treated as classical particles and dynamical effects are neglected. This limits the simulations to zero temperature. While it is possible in principle to calculate the phonon spectrum and even to perform nonzero temperature molecular dynamics, treating the electrons with the rigor of the static calculations reported here, such studies are not feasible at present for systems as complicated as carbonated hydroxyapatite. However, nonzero temperature calculations would be possible with a classical force model such as a shell model. These would give some indication of the effect of lattice vibrations on the atomic arrangements and the lattice parameter, and whether a first principles study would be worthwhile. It would be particularly useful to investigate the effects of hydrogen dynamics in HA itself and in the carbonated materials.

V. Conclusions

Different carbonate substitution mechanisms in bulk hydroxyapatite have been studied by means of first principles simulations. The results show that B- or PO_4-site substitutions are energetically preferred to A- or OH-site substitutions. Qualitative agreement with experiments for the behavior of lattice parameters is found. These results offer a starting point for more comprehensive first principles investigation of natural bone minerals, where the focus will be on understanding solubility, surface chemistry, and biological properties from a physical basis.

Acknowledgment. Work supported by the Natural Sciences and Engineering Research Council of Canada, and Millenium Biologix Corp.

CM050523B